ISSN 1674-1056
http://cpb.iphy.ac.cn
http://iopscience.iop.org/cpb
中国物理 B
Chinese Physics
中国物理 Chinese Physics B

Responsive mechanism and molecular design of di-2-picolylamine-based two-photon fluorescent probes for zinc ions

Mei-Yu Zhu(朱美玉), Ke Zhao(赵珂), Jun Song(宋军), Chuan-Kui Wang(王传奎)
Citation: Chin. Phys. B . 2018, 27(2): 023302. **doi:** 10.1088/1674-1056/27/2/023302

Journal homepage: http://cpb.iphy.ac.cn; http://iopscience.iop.org/cpb

What follows is a list of articles you may be interested in

Temperature dependence of line parameters of $^{12}C^{16}O_2$ near 2.004 μm studied by tunable diode laser spectroscopy

Hongliang Ma(马宏亮), Mingguo Sun(孙明国), Shenlong Zha(查申龙), Qiang Liu(刘强), Zhensong Cao(曹振松), Yinbo Huang(黄印博), Zhu Zhu(朱柱), Ruizhong Rao(饶瑞中)
Chin. Phys. B . 2018, 27(2): 023301. **doi:** 10.1088/1674-1056/27/2/023301

Responsive mechanism of 2-(2'-hydroxyphenyl)benzoxazole-based two-photon fluorescent probes for zinc and hydroxide ions

Zhang Yu-Jin, Zhang Qiu-Yue, Ding Hong-Juan, Song Xiu-Neng, Wang Chuan-Kui
Chin. Phys. B . 2015, 24(2): 023301. **doi:** 10.1088/1674-1056/24/2/023301

TDDFT study of excitation of water molecules with short laser pulses

Wang Zhi-Ping, Wu Ya-Min, Zhang Xiu-Mei, Lu Chao
Chin. Phys. B . 2013, 22(7): 073301. **doi:** 10.1088/1674-1056/22/7/073301

Global analysis of the Comet-tail system of $^{12}C^{16}O^+$

Shao Xu-Ping, Zhao Min, Yang Xiao-Hua
Chin. Phys. B . 2013, 22(7): 073302. **doi:** 10.1088/1674-1056/22/7/073302

The structural and spectroscopic properties for uranium oxides

Li Peng,Jia Ting-Ting,Gao Tao,Li Gan
Chin. Phys. B . 2012, 21(4): 043301. **doi:** 10.1088/1674-1056/21/4/043301

Responsive mechanism and molecular design of di-2-picolylamine-based two-photon fluorescent probes for zinc ions*

Mei-Yu Zhu(朱美玉), Ke Zhao(赵珂)†, Jun Song(宋军), and Chuan-Kui Wang(王传奎)

School of Physics and Electronics, Shandong Normal University, Jinan 250358, *China*

(Received 7 September 2017; revised manuscript received 23 October 2017; published online 5 January 2018)

The properties of one-photon absorption (OPA), emission and two-photon absorption (TPA) of a di-2-picolylamine-based zinc ion sensor are investigated by employing the density functional theory in combination with response functions. The responsive mechanism is explored. It is found that the calculated OPA and TPA properties are quite consistent with experimental data. Because the intra-molecular charge transfer (ICT) increases upon zinc ion binding, the TPA intensity is enhanced dramatically. According to the model sensor, we design a series of zinc ion probes which differ by conjugation center, acceptor and donor moieties. The properties of OPA, emission and TPA of the designed molecules are calculated at the same computational level. Our results demonstrate that the OPA and emission wavelengths of the designed probes have large red-shifts after zinc ions have been bound. Comparing with the model sensor, the TPA intensities of the designed probes are enhanced significantly and the absorption positions are red-shifted to longer wavelength range. Furthermore, the TPA intensity can be improved greatly upon zinc ion binding due to the increased ICT mechanism. These compounds are potential excellent candidates for two-photon fluorescent zinc ion probes.

Keywords: two-photon absorption, fluorescent probe, zinc ion, intra-molecular charge transfer

PACS: 33.20.–t ,42.65.–k, 82.30.Fi **DOI:** 10.1088/1674-1056/27/2/023302

1. Introduction

One of the important applications of two-photon absorption (TPA) materials is the two-photon microscopy (TPM), which employs two near-infrared photons as an excitation source.[1] Compared with the one-photon microscopy, TPM has a lot of advantages including increased penetration depth (>500 μm), low tissue auto-fluorescence and self-absorption, as well as reduced photo-damage and photo-bleaching.[2–4] As such, TPM is very useful for long-term imaging for live tissues. To expand the utility of TPM, there is a strong need to develop a variety of two-photon (TP) probes for specific applications. Recently, the design and synthesis of TP fluorescent probes has become a rapidly emerging field, and then numerous TP probes for diverse analytes, such as cation and anion ions,[5–8] pH values,[9,10] small molecules,[11,12] and DNA[13] have been developed. A powerful TP probe needs to have an efficient TP fluorophore with large TPA cross section.[4] During the last two decades, great efforts have been made to study the structure-property relationships for the design of TP fluorophores. It has been revealed that expansion of π-electron conjugation and enhancement of intra-molecular charge transfer (ICT) will enhance the TPA activities of many organic molecules.[14,15]

Zinc ion is an essential component in enzymes and proteins, and it is involved in many biological processes in the human body.[16–18] To understand the roles of zinc ions in biology, it is crucial to detect them in the live cell and tissues. Nowadays, a number of zinc ions turn-on or ratiometric TP probes have been synthesized and their bioimaging applications have been demonstrated.[5,6] However, the relevant theoretical study is still in the primary stage.[19–23] Wang *et al.*[19] designed a series of Salen-based TP zinc ion probes based on the ICT mechanism. The one-photon absorption (OPA), TPA and fluorescence properties were calculated through the quantum chemical method. It was found that the series of ligands can become fluorescent bioimaging reagents used for ratiometric detection. Bednarska *et al.*[20] elucidated the sensing mechanism for a bipyridine-centered ratiomatric zinc ions probe by computational methods. The electric structure and nonlinear absorption spectra were calculated including solute-solvent interactions. Their work indicated that nonlinear response functions combined with density functional theory (DFT) can successfully be used to analyze metal ion probes. In our previous work,[21] response theory was used to investigate OPA, TPA as well as emission properties of a series of zinc ion and pH sensitive materials. Theoretical study on the relationship between molecular structure and photophysical property has great importance in guiding the exper-

*Project supported by the Shandong Provincial Natural Science Foundation, China (Grant No. ZR2014AM026), the National Natural Science Foundation of China (Grant Nos. 11374195 and 11404193), and the Taishan Scholar Project of Shandong Province, China.

†Corresponding author. E-mail: zhaoke@sdnu.edu.cn

© 2018 Chinese Physical Society and IOP Publishing Ltd

imental design and synthesis of TP probes. At the same computational level, the optical properties of different compounds can be compared accurately.[24–28]

In this work, we choose a di-2-picolylamine (DPA)-based Zn^{2+} ion TP probe as a model molecule. It has been reported that this probe undergoes significant increase of the TPA cross section by the Zn^{2+} coordination.[29] To explore the recognition mechanism of the probe, we perform a theoretical study on the OPA, emission and TPA properties of the probe before and after combination with Zn^{2+} at the DFT level. At the same time, on the basis of the model probe, making good use of the influences of the π-conjugation center and the electronic donor and acceptor moieties on TPA properties, a series of DPA-based TP zinc ion probes are designed and their linear and nonlinear optical properties are computed. The intent of the design is to achieve the TP probes having not only the large TPA cross section but also the significant TPA enhancement upon zinc ion coordination. The structure-property relationships and the responsive mechanisms are discussed at length. Our research will provide useful guidelines for designing and synthesizing the TP probes for metal ions.

2. Computational method

The OPA strength between the ground $|0\rangle$ and the excited $|f\rangle$ states can be described by the oscillator strength

$$f_{\mathrm{op}} = \frac{2\omega_f}{3}\sum_{\alpha}|\langle 0|\mu_\alpha|f\rangle|^2, \tag{1}$$

where $\alpha \in (x,y,z)$, μ_α is the dipole moment operator, and ω_f denotes the excitation energy.

The TPA cross section can be obtained by calculating the individual TP transition matrix elements $S_{\alpha\beta}$ between the initial state $|0\rangle$ and final state $|f\rangle$[30]

$$S_{\alpha\beta} = \sum_s \left(\frac{\langle 0|\,\mu_\alpha\,|s\rangle\,\langle s|\,\mu_\beta\,|f\rangle}{\omega_s - \omega} + \frac{\langle 0|\,\mu_\beta\,|s\rangle\,\langle s|\,\mu_\alpha\,|f\rangle}{\omega_s - \omega} \right), \tag{2}$$

where α, $\beta \in (x,y,z)$, ω is the fundamental frequency of the laser beam and assumed to be equal to half of the excitation energy of the final state, i.e., $2\omega = \omega_f$, and ω_s represents the excitation energy for the intermediate state $|s\rangle$. The summation here includes all intermediate, initial and final states. In response theory, the two-photon matrix element $S_{\alpha\beta}$ can be calculated through the single residues of the quadratic response function.[31]

The microscopic TPA cross section of molecules excited by a linearly polarized single beam can be expressed as[30,32]

$$\delta = \sum_{\alpha,\beta}(2S_{\alpha\alpha}S^*_{\beta\beta} + 4S_{\alpha\beta}S^*_{\alpha\beta}). \tag{3}$$

The macroscopic TPA cross section that can be directly compared with the experimental measurement, is defined as[32]

$$\sigma = \frac{4\pi^2 a_0^5 \alpha\omega^2}{15c\Gamma}\delta. \tag{4}$$

Here a_0 is the Bohr radius, c is the speed of light, α is the fine structure constant, Γ is the level broadening of the final state and is assumed to have the commonly used value $\Gamma = 0.1$ eV. The TPA cross section is in units of GM (1 GM = 10^{-50} cm^4·s/photon).

In this work, the geometrical structures of ground states are fully optimized by using DFT with the 6-31G(d,p) basis set and the B3LYP hybrid functional. On the basis of the optimized structures, the OPA properties are computed by the time-dependent DFT (TD-DFT) approach at the B3LYP level with the 6-31G(d) basis set. The first excited state geometry optimization and fluorescence properties are calculated by using the TD-DFT at the same level. All the calculations of optimization, OPA and emission properties are carried out in the Gaussian 09 program.[33] The TPA cross sections are obtained by response theory through using the B3LYP functional with the 6-31G(d) basis set in the Dalton 2013 package.[34] In addition, the effect of the water solvent is taken into account with the self-consistent reaction field theory by means of the polarizable continuum model (PCM) in both Gaussian and Dalton calculations. Our previous work has shown that the B3LYP functional calculations can give reasonable TPA properties which are consistent with the trend of experimental observations.[24–28] The use of the pseudo potential basis sets could probably provide better numerical results, but we believe that the overall picture would not change.

3. Results and discussion

3.1. Molecular design and geometry optimization

The chemical structure for the model probe 1 is depicted in Fig. 1. Probe 1 uses 2-acetyl-6-dimethylamino naphthalene (acedan) as the fluorophore, and DPA as the Zn^{2+} receptor. It has been shown that acedan derivatives possess a significant TPA cross section and have been widely used to design TP cation sensors.[35] The receptor DPA is connected with the acyl moiety which is the electron acceptor of acedans. Hence, the acetyl group could be involved in coordination with Zn^{2+}. The 1Zn is the corresponding coordination structure where the oxygen atom participates in the coordination and all of the three nitrogen atoms of the DPA group are chelated to Zn^{2+}. In experiment, the measurements are performed in aqueous solutions containing NaCl. So the Cl^- environment is considered explicitly. Our later calculations show that the introduction of the two Cl^- ions can provide the reasonable excitation energies in comparison with the experimental values.

For designing efficient TP fluorophore, one needs to consider the established TPA structure-property relationships. It has been revealed that a number of key structural factors, such as the electron richness and planarity of the π-conjugation center, the molecular symmetry, the strength of donor and acceptor, as well as the conjugated length and dimensionality, play important roles in enhancing the TPA activities.

On the basis of the model probe, at first, we design two new structures 2 and 3 by using acyl moiety and the DPA receptor as shown in Fig. 1. By inspecting the structure of probe 1, one can notice that the naphthalene part has good planarity which can facilitate the charge transfer. However, its conjugated length is too short. In order to improve the TPA intensity, the conjugation center is replaced by the distyrylbenzene group in probe 2. The distyrylbenzene has been widely used in TPA materials. When the distyrylbenzene center is connected with electron donor or acceptor terminals, the system exhibits a strong TPA response.[36] In probe 3, the DPA receptor is combined with the benzene ring directly, while the acyl moiety is attached to the side of the conjugated center. The corresponding zinc complex 3Zn could also realize the coordination between the Zn^{2+} ion and the oxygen atom. It would be very interesting to see how different the TPA spectra of probes 2 and 3 are.

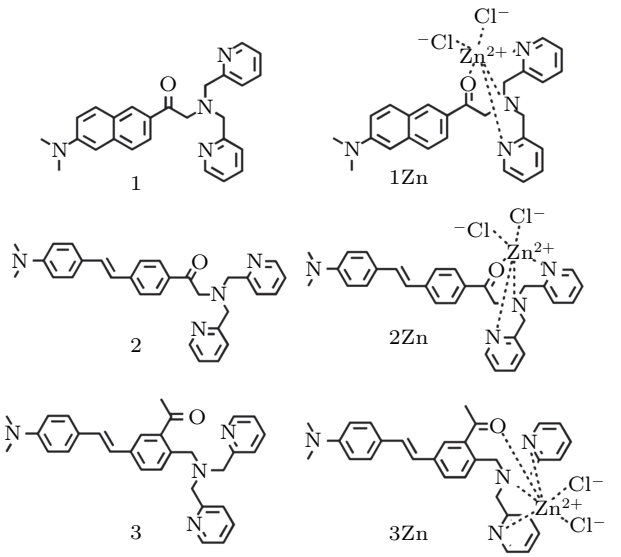


Fig. 1. Chemical structures of probes 1, 2, 3 and the corresponding zinc complexes.

The optimized geometries of these three probes and their zinc complexes are illustrated in Fig. 2. The frequency calculations for these geometries do not produce any imaginary frequencies. It is found that all the backbones have good planarity. The Zn^{2+} ion can chelate both the DPA receptor and the acyl moiety in all cases. The bond length between the oxygen or nitrogen atom and Zn^{2+} ion has a typical value of 2.1 Å–2.3 Å, which is similar to the x-ray crystal structure.[29] The permanent dipole moments have also been examined and the results reveal that the dipole moments of 1Zn, 2Zn, and 3Zn are 21.03 D, 21.93 D, and 25.65 D respectively, which are about 2.5–3.5 times larger than the values of the corresponding free ligands.

Then, employing pyridine and DPA, we design another group of probes 4–6. The chemical formulas are given in Fig. 3. The pyridine is often used in TPA active chromophores and acts as an electronic acceptor. To guarantee a large TPA response, all the fluorophores in these designed probes have the donor-π-acceptor structures. In probe 5, a cyano group is added to the pyridine in order to enhance the acceptor strength. On the basis of probe 5, probe 6 is generated by replacing the dimethylamino terminal with the diphenylamine because the diphenylamine group has stronger ability to donate and transport electrons. For this group of designed probes, the pyridine can act both as an electron acceptor of the fluorophore and as a recognition site for zinc ions. Therefore, the zinc complexes are supposed to yield increased TPA cross sections in comparison with the corresponding free ligands.

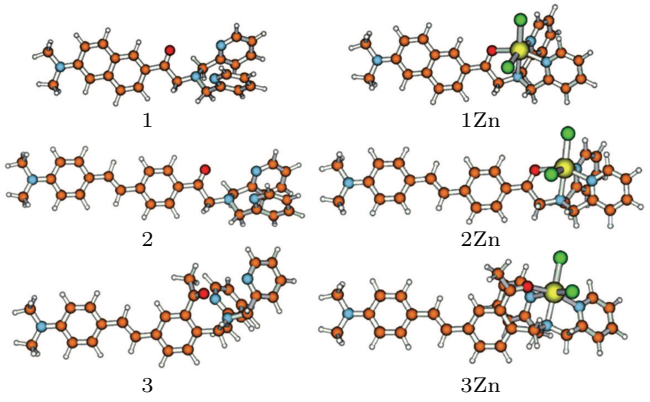


Fig. 2. (color online) Optimized geometries of probes 1, 2, 3, and the corresponding zinc complexes.

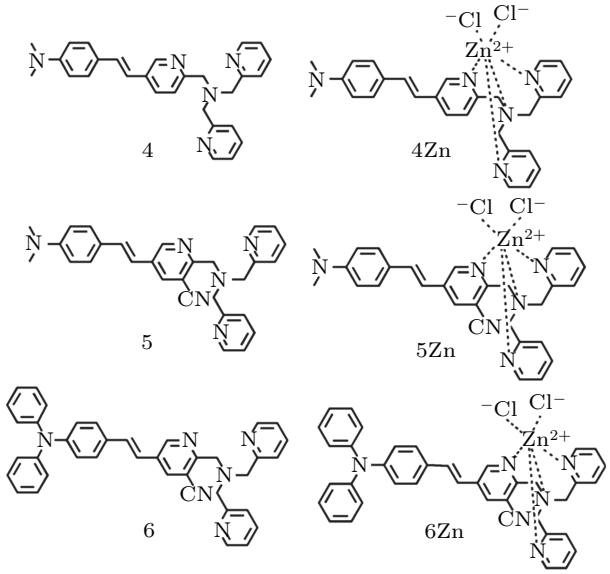


Fig. 3. Chemical structures of probes 4, 5, 6 and the corresponding zinc complexes.

The optimized geometries of the designed probes 4–6 and their zinc complexes are presented in Fig. 4. It is noticed that each of all the studied systems has a nearly planar center. For the zinc complex, the nitrogen atom in central pyridine can really participate in coordination, together with the three nitrogen atoms of the DPA receptor. The coordination bond lengths are also in a range of 2.1 Å–2.3 Å and the metal binding leads to a great increase in the dipole moment. It should be mentioned that the introduction of the cyano group could affect the binding sites of Zn^{2+} ions for the 5Zn and 6Zn molecules. The Zn^{2+} ions could coordinate with the nitrogen atom of the cyano group. We also try to optimize 5Zn and 6Zn with different initial conformations, but the convergent geometries in which the zinc ion coordinates with both the DPA receptor and the nitrogen atom of the cyano group are not obtained.

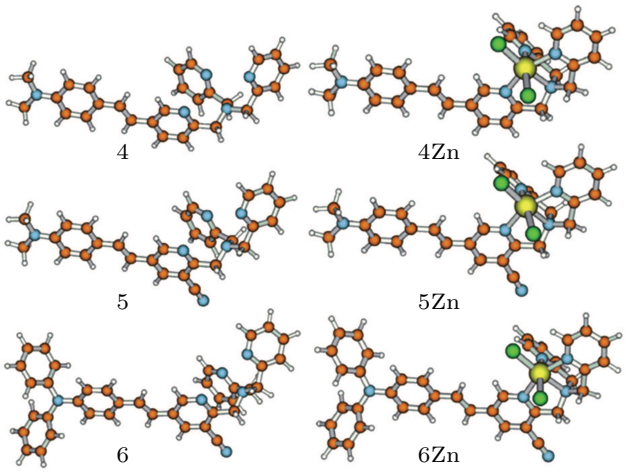


Fig. 4. (color online) Optimized geometries of probes 4, 5, 6, and the corresponding zinc complexes.

3.2. One-photon absorption and emission properties

The experimental linear absorption peak of the probe 1 is centered at around 374 nm with a broad band. After it coordinates with Zn^{2+} ions, the absorption shifts in the visible light range 400 nm–450 nm.[29] The emission wavelength of the probe is observed at 546 nm and has a red-shift of 24 nm due to the titration of the Zn^{2+} ions.

Our calculated OPA wavelength λ_{op}, oscillator strength f_{op} and transition nature of all the studied molecules are listed in Table 1. One can see that λ_{op} of 1 is located at 377 nm, which is in very good agreement with the experimental value. When the molecule binds to zinc ions, λ_{op} is red-shifted greatly to 417 nm. The red-shift comes to 40 nm. This result is also quite consistent with the experimental observations, indicating that the B3LYP functional is suitable for our calculations. In comparison with 1, λ_{op} values of all the designed probes are red-shifted significantly because of the extending conjugated center and strong acceptor and donor. The λ_{op} values of probes 2, 5, and 6 reach up to 448 nm, 435 nm, and 444 nm respectively, which means that the fluorophores in these molecules are more beneficial to charge transfer. It should be mentioned that most of the TP probes which are based on acedan and its derivatives show the maximum OPA wavelength around 370 nm. This would cause limited penetration, substantial auto-fluorescence and photon-bleaching in tissue imaging under the TP excitation.[3] Therefore, there is a strong need to design new TP probes that can be excited at longer wavelengths. From Table 1, one can notice that upon Zn^{2+} binding, λ_{op} of the first excited state has a large red-shift for all probes. The red-shifts of 2Zn and 3Zn are equal to 60 nm and 88 nm. The red-shifts of 4Zn, 5Zn and 6Zn are 18 nm, 37 nm, and 34 nm, respectively. The transition nature shows that the maximum OPA peaks of these molecules are mostly derived from the transition between the ground state (S_0) and the first excited state (S_1) which is mainly dominated by the transition from the highest occupied molecular orbital (HOMO) to the lowest unoccupied molecular orbital (LUMO). But OPA peaks of 3Zn and 5Zn are related to the second excited state (S_2) transition dominated by the transition from HOMO to LUMO+1.

Table 1. One-photon absorption and emission properties of the molecules.

	λ_{op}/nm	f_{op}	Transition nature	λ_{em}/nm	f_{em}	Transition nature
1	377	0.54	S_0–S_1 H–L(95%)	423	0.70	S_1–S_0 H–L(98%)
1Zn	417	0.69	S_0–S_1 H–L(97%)	484	0.80	S_1–S_0 H–L(98%)
2	448	1.27	S_0–S_1 H–L(99%)	524	1.67	S_1–S_0 H–L(99%)
2Zn	508	1.28	S_0–S_1 H–L(97%)	599	1.55	S_1–S_0 H–L(99%)
3	391	1.12	S_0–S_1 H–L(98%)			
3Zn	479	0.10	S_0–S_1 H–L(98%)			
	398	1.02	S_0–S_2 H–L+1(97%)			
4	388	1.20	S_0–S_1 H–L(99%)	467	1.61	S_1–S_0 H–L(99%)
4Zn	406	1.01	S_0–S_1 H–L(98%)	479	1.43	S_1–S_0 H–L(99%)
5	435	0.51	S_0-S_1 H–L(94%)	509	0.63	S_1–S_0 H–L(99%)
5Zn	472	0.27	S_0–S_1 H–L(89%)	583	0.17	S_1-S_0 H–L(99%)
	424	0.78	S_0–S_2 H–L+1(89%)			
6	444	0.89	S_0–S_1 H–L(99%)	530	1.14	S_1–S_0 H–L(99%)
6Zn	478	0.64	S_0–S_1 H–L(98%)	558	0.93	S_1–S_0 H–L(99%)

The geometry optimization for the first excited state on the basis of the ground state geometries is carried out by the TD-DFT method at the B3LYP level with the 6-31G(d,p) basis set in water solvent. The obtained fluorescence emission wavelength λ_{em}, corresponding oscillator strength f_{em} and transition nature are also given in Table 1. On going from free ligand to zinc complex, λ_{em} of 1Zn is shifted from 423 nm to 484 nm. This is consistent with the trend of the experimental data. The shifts of 2Zn and 5Zn are very large and the values come to 75 nm and 74 nm respectively. The results demonstrate that these probes are suitable for the ratiometric measurement. Compared with λ_{op}, λ_{em} values of all the molecules also have large red-shifts. It has been known that the large Stokes shift is helpful in avoiding the interference of absorption and emission spectra and improving the sensitivity and accuracy of the detection. One can also notice that the difference between the fluorescence emission wavelengths λ_{em} of 6Zn and probe 6 is only 28 nm, which could lead to a lower sensitivity to identify zinc ions.

3.3. Two-photon absorption

The TPA wavelength λ and cross section σ in water solvent for all the studied molecules are calculated by the response theory. The simulated TPA spectra with Lorentz broadening for the first group molecules are illustrated in Fig. 5. We pay attention to the TPA behavior at the two-photon wavelengths above 700 nm, where the lowest excited electronic states are located. For probe 1, the first excited state has the largest TPA cross section, which produces one absorption peak in the spectrum. The value of σ is equal to 138 GM at 756 nm, which is very close to the experimental value, 133 GM at 800 nm.[29] When the probe coordinates with Zn^{2+}, λ shifts to 844 nm and σ increases up to 237 GM. In experiment, the TPA peak of the zinc complex is centered at 840 nm and the cross section increases to 205 GM. Therefore, our TPA calculations are in very good agreement with experimental data. Looking at the designed molecules, one can see that probe 2, 2Zn and probe 3 each have one absorption peak corresponding to the first excited state, while 3Zn has two separated peaks with different intensities due to the large σ values of both the first and second excited states. The peak position of probe 2 is at 919 nm and has a large red-shift of 163 nm with respect to that of probe 1. The peak value of probe 2 is 1092 GM, which is much higher than that of probe 1. This demonstrates that the distyrylbenzene is an excellent conjugated center for enhancing TPA in a longer wavelength range. As mentioned above, there is a strong need to develop the new TP probe that can be excited at longer wavelength ($>$ 900 nm). Hence, the molecule 2 is a good candidate for the TP probe in this wavelength domain. Upon Zn^{2+} binding, the peak position of 2Zn is red-shifted to 1052 nm and the maximum cross section increases dramatically to 1607 GM. The increase is about 50%. As for probe 3, λ is blue-shifted and σ decreases with respect to that of probe 2 due to the side position of the acceptor. In the case of 3Zn, two strong absorption bands appear at about 816 nm and 966 nm with the cross sections of 466 GM and 227 GM. We attribute this observation to the increased dimensionality of the charge transfer channel. It can be concluded that the metal binding gives rise to important effects on the TPA wavelength and cross section.

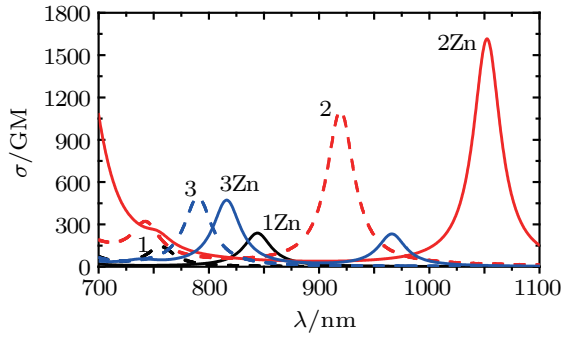


Fig. 5. (color online) TPA spectra of probes 1, 2, 3 and the corresponding zinc complexes.

As is well known, TPA properties strongly depend on the ICT process. The charge in a molecule will be redistributed when the system is excited from the ground state to the excited state. In order to explore the responsive mechanism and obtain a better understanding of the ICT process, we perform the natural bond orbital charge analyses for probes 1 and 2, as well as their zinc complexes in the ground states and in the first excited states. To analyze them clearly, these molecules are divided into four parts as shown in Fig. 6. The net charges of parts A, B, C and D are specifically calculated and all the calculated results are listed in Table 2.

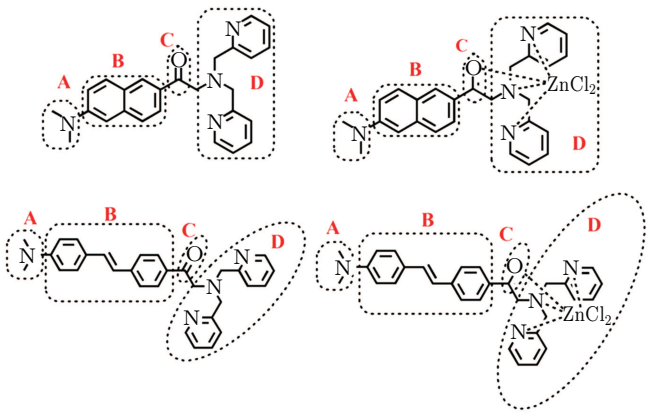


Fig. 6. (color online) Divided parts of the probe 1, 1Zn, probe 2, and 2Zn.

Table 2. Net charges (in units of e) for divided parts of the molecules in the ground states and in the first excited states.

	Q_{A0}	Q_{A1}	ΔQ_A	Q_{B0}	Q_{B1}	ΔQ_B	Q_{C0}	Q_{C1}	ΔQ_C	Q_{D0}	Q_{D1}	ΔQ_D
1	0.031	0.244	0.213	0.014	0.007	–0.007	–0.030	–0.212	–0.182	–0.015	–0.039	–0.024
1Zn	0.056	0.240	0.184	0.101	0.173	0.072	–0.047	–0.232	–0.185	–0.110	–0.181	–0.071
2	0.026	0.214	0.188	0.007	0.013	0.006	–0.022	–0.182	–0.160	–0.012	–0.045	–0.033
2Zn	0.038	0.224	0.186	0.103	0.161	0.058	–0.035	–0.215	–0.180	–0.106	–0.170	–0.064

Q_{A0} and Q_{A1} denote the net charge of part A in the ground state and the first excited state, respectively; ΔQ_A represents the net charge difference of part A between the ground state and the first excited state. Like this definition, ΔQ_B, ΔQ_C, and ΔQ_D denote the net charge differences of part B, part C and part D between the ground state and the first excited state. For probe 1, it is found that the net charge of part A in the first excited state Q_{A1} is $0.244e$, which is more electropositive than the value in the ground state Q_{A0}, $0.031e$. The ΔQ_B is so small that it can be neglected. The net charge of part C in the first excited state (Q_{C1}, $-0.212e$) is more electronegative than in the ground state (Q_{C0}, $-0.03e$). The case of part D is the same as that of part C. This indicates that part A is the donor of the molecule and part C, together with part D, is the acceptor of the molecule. For 1Zn, part A and part B act as the donors and part C and part D behave as the acceptors. The net charge difference of the donor should be the sum of ΔQ_A and ΔQ_B, $0.256e$, which is larger than ΔQ_A of 1 ($0.213e$). This demonstrates that the ICT increases upon metal binding. Like the cases of 1 and 1Zn, the net charge difference of donor in 2Zn is the sum of ΔQ_A and ΔQ_B, $0.244e$, which is larger than the corresponding value in molecule 2, $0.194e$. The ICT also increases after it coordinates with the Zn^{2+} ion.

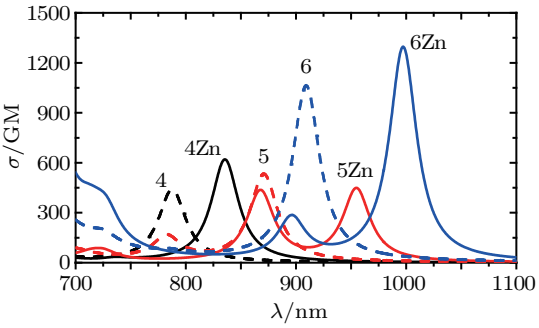


Fig. 7. (color online) TPA spectra of probes 4, 5, 6 and the corresponding zinc complexes.

The simulated TPA spectra for the second group molecules are plotted in Fig. 7. It shows that the spectra of all the molecules each have a TPA peak at different positions expect for 5Zn. The spectral shape of 5Zn has a pattern characterized by two absorption bands with comparative intensities. The largest cross section of probe 4 is located at 788 nm. Compared with experimental probe 1, the absorption intensity is enhanced 3-fold from 138 GM to 436 GM. Upon zinc ion coordination, the absorption wavelength of 4Zn is red-shifted to 836 nm and the absorption intensity is raised to 618 GM. In comparison with probe 4, as expected, adding a cyano group leads to a little increase of the TPA cross section for molecule 5 due to the enhanced acceptor strength. The peak value of probe 5 becomes 522 GM, while the effect on the TPA wavelength is large. The peak position of probe 5 is red-shifted to 871 nm. The intensities of two absorption bands of 5Zn are 436 GM and 422 GM centered at 955 nm and 868 nm respectively. When looking at the case of probe 6, in which the stronger donor group is used, we can find that the absorption wavelength is longer than 900 nm and the absorption intensity reaches up to 1046 GM. After the probe combines with Zn^{2+}, the peak position occurs at around 1000 nm and the cross section comes to 1285 GM.

4. Conclusions

The OPA, emission and TPA properties of a DPA-based TP fluorescent sensor before and after combination with Zn^{2+} ion are theoretically studied at a DFT level. The ICT mechanism is specified. The calculated OPA and TPA wavelengths and TPA cross sections are in very good agreement with the experimental observations. The OPA and TPA wavelengths show dramatic red-shifts and the TPA cross section is enhanced greatly due to the increased ICT mechanism upon metal binding. On the basis of the experimental probe, we design a series of probes employing different π-conjugation centers, electron acceptors and donors, which can improve the TPA response. The established structure-property relationship is taken into account. The OPA, emission and TPA properties of these designed probes are calculated. It is found that all of the designed probes can achieve the coordination between the acceptor and Zn^{2+} ion. The OPA and emission wavelengths of the designed probes have large red-shifts after metal ion has been bound, which demonstrates that the designed probes are suitable for ratiometric detection. As expected, all of the designed probes have larger TPA cross sections at longer wavelength ranges. The designed probes 2 and 6 are good candidates for the TP probes that can be excited at the wavelengths above 900 nm. Moreover, the TPA cross sections are enhanced significantly after the metal ion has been bound. It should be realized that the enhanced ICT is sometimes accompanied by

a reduction in the fluorescence quantum yield.[4] There is a trade-off between the TPA cross section and the fluorescence quantum yield. These two aspects determine the brightness of the fluorescence emission in real applications and should be considered simultaneously. Our results provide useful guidelines for designing the efficient ratiometric TP probes for metal ions.

References

[1] Denk W, Strickler J H and Webb W W 1990 *Science* **248** 73
[2] Yao S and Belfield K D 2012 *Eur. J. Org. Chem.* **2012** 3199
[3] Kim D, Ryu H G and Ahn K H 2014 *Org. Biomol. Chem.* **12** 4550
[4] Kim H M and Cho B R 2015 *Chem. Rev.* **115** 5014
[5] Kim H M and Cho B R 2011 *Chem. Asian J.* **6** 58
[6] Sarkar A R, Kang D E, Kim H M and Cho B R 2014 *Inorg. Chem.* **53** 1794
[7] Sumalekshmy S and Fahrni C J 2011 *Chem. Mater.* **23** 483
[8] Kim D, Singha S, Wang T, Seo E, Lee J H, Lee S J, Kim K H and Ahn K H 2012 *Chem. Commun.* **48** 10243
[9] Kim H M, An M J, Hong J H, Jeong B H, Kwon O, Hyon J Y, Hong S C, Lee K J and Cho B R 2008 *Angew. Chem. Int. Ed.* **47** 2231
[10] Kim H J, Heo C H and Kim H M 2013 *J. Am. Chem. Soc.* **135** 17969
[11] Das S K, Lim C S, Yang S Y, Han J H and Cho B R 2012 *Chem. Commun.* **48** 8395
[12] Masanta G, Heo C H, Lim C S, Bae S K, Cho B R and Kim H M 2012 *Chem. Commun.* **48** 3518
[13] Zhang Y, Wang J, Jia P, Yu X, Liu H, Liu X, Zhao N and Huang B 2010 *Org. Biomol. Chem.* **8** 4582
[14] Pawlicki M, Collins H A, Denning R G and Anderson H L 2009 *Angew. Chem. Int. Ed.* **48** 3244
[15] Kim H M and Cho B R 2009 *Chem. Commun.* **0** 153
[16] Bush A I, Pettingell W H, Multhaup G, Paradis M d, Vonsattel J P, Gusella J F, Beyreuther K, Masters C L and Tanzi R E 1994 *Science* **265** 1464
[17] Cuajungco M P and Lees G J 1997 *Neurobiol. Dis.* **4** 137
[18] Bush A I and Tanzi R E 2002 *Proc. Natl. Acad. Sci. USA* **99** 7317
[19] Wang D, Guo J F, Ren A M, Huang S, Zhang L and Feng J K 2014 *J. Phys. Chem. B* **118** 10101
[20] Bednarska J, Zaleśny R, Murugan N A, Bartkowiak W, Ågren H and Odelius M 2016 *J. Phys. Chem. B* **120** 9067
[21] Zhang Y J, Zhang Q Y, Ding H J, Song X N and Wang C K 2015 *Chin. Phys. B* **24** 023301
[22] Huang S, Yang B Z, Jiang X F and Ren A M 2016 *J. Mol. Model.* **22** 34
[23] Mukherjee T, Pessoa J C, Kumar A and Sarkar A R 2012 *Dalton Trans.* **41** 5260
[24] Zhao K, Liu P W, Wang C K and Luo Y 2010 *J. Phys. Chem. B* **114** 10814
[25] Wang F Q, Zhao K, Zhu M Y and Wang C K 2016 *J. Phys. Chem. B* **120** 9708
[26] Wu X L, Zhao K, Jia H H and Wang F Q 2015 *Acta Phys. Sin.* **64** 233301 (in Chinese)
[27] Zhao K, Han G C, Zhang L L and Jia H H 2014 *Chin. J. Chem. Phys.* **27** 75
[28] Jia H H, Zhao K and Wu X L 2014 *Chem. Phys. Lett.* **612** 151
[29] Xue L, Fang Z, Li G, Wang H and Jiang H 2011 *Sens. Actuator B-Chem.* **156** 410
[30] Luo Y, Norman P, Macak P and Ågren H 2000 *J. Phys. Chem. A* **104** 4718
[31] Olsen J and Jørgensen P 1985 *J. Chem. Phys.* **82** 3235
[32] Monson P R and McClain W M 1970 *J. Chem. Phys.* **53** 29
[33] GAUSSIAN 09, References in http://www.gaussian.com/
[34] DALTON 2013 *A molecular electronic structure program*, Release *Dalton*2013.0, see http://daltonprogram.org/
[35] Kim H M and Cho B R 2009 *Acc. Chem. Res.* **42** 863
[36] Zhao K, Ferrighi L, Frediani L, Wang C K and Luo Y 2007 *J. Chem. Phys.* **126** 204509